Fatigue damage observed non-destructively in fibre composite coupon test specimens by X-ray CT

Jespersen, Kristine Munk; Mikkelsen, Lars Pilgaard

Published in:
I O P Conference Series: Materials Science and Engineering

Link to article, DOI:
10.1088/1757-899X/139/1/012024
10.1088/1757-899X/139/1/012024

Publication date:
2016

Document Version
Publisher's PDF, also known as Version of record

Fatigue damage observed non-destructively in fibre composite coupon test specimens by X-ray CT

2016 IOP Conf. Ser.: Mater. Sci. Eng. 139 012024

(http://iopscience.iop.org/1757-899X/139/1/012024)

IOP Conf. Series: Materials Science and Engineering **139** (2016) 012024 doi:10.1088/1757-899X/139/1/012024

Fatigue damage observed non-destructively in fibre composite coupon test specimens by X-ray CT

K M Jespersen[1] **and L P Mikkelsen**

Department of Wind Energy, Section of Composites and Materials Science, Technical University of Denmark, Risø Campus, 4000 Roskilde, DK

E-mail: kmun@dtu.dk[1]

Abstract. This study presents a method for monitoring the 3D fatigue damage progression on a micro-structural level in a glass fibre/polymer coupon test specimen by means of laboratory X-ray Computed Tomography (CT). A modified mount and holder made for the standard test samples to fit into the X-ray CT scanner along with a tension clamp solution is presented. Initially, the same location of the test specimen is inspected by ex-situ X-ray CT during the fatigue loading history, which shows the damage progression on a micro-structural level. The openings of individual uni-directional (UD) fibre fractures are seen to generally increase with the number of cycles, and new regions of UD fibre fractures also appear. There are some UD fibre fractures that are difficult to detect since their opening is small. Therefore, the effect of tension on the crack visibility is examined afterwards using a tension clamp solution. With applied tension some additional cracks become visible and the openings of fibre fractures increases, which shows the importance of applied tension during the scan.

1. Introduction

Wind power turbines are increasingly used in many parts of the world to match the increasing demand for sustainable energy. Among sustainable energy sources wind power is one of the most cost efficient technologies, however they are yet to be competitive to fossil fuels. The cost of energy can be decreased by increasing the blade length, as the power output of the wind turbine scales with the blade length squared. One of the main design factors when increasing the length of the blade is material fatigue, since the blades experience a high degree of repeated loading [1]. The wind variation causes the blades to bend in the direction of the tower (flap-wise bending), and the rotation results in the gravitational loads of the blades repeatedly changing direction causing a repeated edge-wise bending motion. With a life-time in the range of 20-30 years the total number of load cycles sums up to 10^8-10^9, which is significantly higher than for e.g. airplanes and cars [2]. Furthermore, it is the degradation of the stiffness rather than the strength which is a concern for wind turbine blades, since the blades might risk hitting the tower. As the blades mainly experience bending loads, uni-directional glass fibre composites made from non-crimp fabrics (NCFs) are commonly used for the load carrying parts of the blades. However, the fatigue mechanism in these NCF composites is not well understood. If the damage mechanism was properly understood on a micro-structural level it would be possible to decrease safety factors and make more fatigue resistant wind turbine blade materials. Therefore, establishing a method capable of monitoring tension-tension fatigue damage progression in a glass fibre/polymer is the focus of this paper.

Fatigue damage progression in composites is a complex process which includes several interacting damage mechanisms. Many of the damage features are small and difficult to monitor non-destructively. The UD NCF composites used for wind turbine blades commonly include cross-crossed thin supporting bundles (backing bundles) to which the UD bundles are stitched to keep them aligned during manufacturing and handling. For these NCF composites the stiffness degradation during fatigue is mainly caused by UD fibre fractures and is also slightly affected by the initial off-axis cracking in the backing bundles. Furthermore, the location of the UD fibre fractures seems to be highly related to the cross-over points of the off-axis backing bundles [3, 4]. Therefore, the damage appears as local fibre fracture regions at various locations rather than purely homogeneously throughout the material. Furthermore, the fibre fractures and off-axis cracks are features of a few micrometers in size and appear as 3D features such as clusters and chains of fibre fractures [4]. All of this makes it difficult to monitor the damage over time experimentally, since a high resolution non-destructive 3D damage monitoring technique is necessary.

Through time, different methods for in-situ damage monitoring have been used in the attempt to monitor damage progression of fibre composites. On a structural level, several methods such as vibraction analysis, acoustic emission, ultrasonic testing [5], and optical sensors [6] techniques have been used to monitor damage in wind turbine blades, however at a millimeter or even centimeter spatial resolution. 2D imaging methods such as SEM and camera imaging have been used to observe the surface damage progression on a micro-structural level [7, 8], and particularly SEM gives invaluable information on small-scale damage mechanisms due to the high resolution. However, using such methods one does not know what happens below the considered surface. In relation to monitoring the damage progression in fibre composites on a micro-structural level in 3D, X-ray Computed Tomography (CT) is probably the most promising technique. Synchrotron radiation CT has due to the short scan times been used for in-situ studies on fibre composites [9, 10, 11, 12]. However, in relation to fatigue damage progression these studies are limited to a few thousand cycles (e.g. [11, 12]) due to the limited access time. Although the scan time is considerably longer, the obtainable resolution for laboratory X-ray CT imaging has recently become competitive to synchrotron CT. Some studies [13, 14, 15] have considered in-situ damage monitoring in composites by laboratory X-ray CT. However, general for most of the studies is that they consider small sample sizes to obtain a high resolution. As considering in-situ loading of down-sized samples might affect the damage mechanisms in the sample, it is of interest to be able to monitor the damage non-destructively in the regular coupon test specimens, which is scope of the current study.

Our work outlines a method capable of monitoring tension fatigue damage in 3D for a glass fibre/polymer coupon test specimen non-destructively by means of laboratory X-ray CT. Modified solutions for mounting the large samples in the X-ray CT scanner and a method to apply tension to the sample during scanning are explained. Furthermore, the study outlines some limitations and some important factors to take into account when evaluating the results.

2. Composite material and test specimens

The considered material is a glass fibre/epoxy composite made from two types of non-crimp fabrics (NCF); a UD and a biax fabric. In the UD fabric thin supporting off-axis backing bundles are stitched to the UD bundles to keep them aligned. The stacking sequence is $[\pm 45,\mathrm{b}/0,\mathrm{b}/0]_s$ where "0" is the UD bundle layer and "b" symbolises the backing layer containing both $\pm 45^\circ$ and 90° fibre bundles. This means that the composite contains 4 layers of UD and has a layer of biax at each surface. The material is similar to that considered in [16].

Plates of the UD laminate were cut into butterfly shaped test specimens (for more information on the specimen geometry, see [17]). The specimen geometry with curved edges is specially designed to test UD composites, as the standard plane geometries tend to fail by shear failure

in the tabs [17]. The specimen length was 410mm, the width of the gauge section was 15mm, and the thickness of the composite was 4.5mm. 140mm long tapered tabs were attached in both ends of the sample.

3. Experimental methods

To investigate the damage progression in the composite, an ex-situ X-ray CT start-stop fatigue test was performed on a full-size butterfly coupon specimen. Every time the test was interrupted the sample was inspected in the same location using X-ray CT, thereby observing the damage progression in terms of individual UD fibre fractures. The influence of applied tension during X-ray CT scanning was examined by a tension clamp solution.

3.1. Fatigue testing

Fatigue tests were performed on a hydraulic Instron test machine (max 250kN) in load control with a sinusodial waveform and a stress ratio of R=0.1. The fatigue test was carried out with a test frequency of 5Hz and the strain was monitored with two extensometers (one on each side of the sample). Two initial static tests were performed on the sample prior to the fatigue test to determine the initial Young's modulus. This was used to determine the load range where a peak strain of 1% was obtained. The sample used for the ex-situ test was stopped four times (after 47300, 57300, 67300, and 77300 cycles) during the fatigue load history for X-ray CT scanning. Another sample was stopped after 67000 cycles, where damage was expected to be present, for investigation of the effect applied tension on the crack visibility.

3.2. X-ray computed tomography

The X-ray CT experiments were carried out on a Zeiss Xradia Versa 520 scanner, using a 2000x2000 pixel detector with a pixel depth of 16 bit. All scans were performed with a binning of 2 of the pixels on the detector. This means that 2x2 pixels are combined into one giving a higher intensity (shorter scan time) but also a larger pixel size (lower resolution). Three different scan settings were used as shown in Table 1. To locate the damage initially in the ex-situ study, a large field of view (LFOV) scan was performed on the sample. After 47300 cycles, it was possible to see an indication of damage despite the coarse resolution ($17.4\mu m$ voxel size). A high resolution scan was then performed in that region by means of the "Scout-and-Scan" principle provided by Zeiss and using the "ex-situ" scan settings labeled "ES" in Table 1. For the remaining times the test was interrupted only high resolution scans were performed. For the tension clamp experiments elaborated later, the scan settings "TC" were used and include a higher number of projections to make up for presence of two carbon pins necessary to transfer the load.

Table 1. X-ray CT scan settings used for the large field of view (LFOV), ex-situ (ES), and tension clamp (TC) scans.

Scan name	Source to sample (mm)	Detector to sample (mm)	Exp. time (s)	No. of projections -	Accelerating voltage (keV)	Pixel size (μm)	Optical Mag.	Scan time (h)
LFOV	30	88	2	801	60	17.4	0.4x	2
ES	28	35	7	4601	70	3	4x	11
TC	30	50	12	5201	70	2.5	4x	20

Because of the large sample size mounting in the scanner is not possible with the standard mount and sample holders. Therefore, a short mount was manufactured and a grip (Makro Grip 5-Achs-Spanner from Lang) was modified to fit into the scanner. Fig. 1 a shows the sample placed in the scanner using the short mount and special sample holder. Using this setup it is possible to scan a bit more than the bottom half of the 410mm long sample (there is a limitation of how far down the sample can go). Furthermore, the sample can be mounted in the same way every time with a variation of less than 1mm. A fine tuning of the location was done by comparing the 2D projection images to ensure as little variation as possible between the location of the observed region in the ex-situ study.

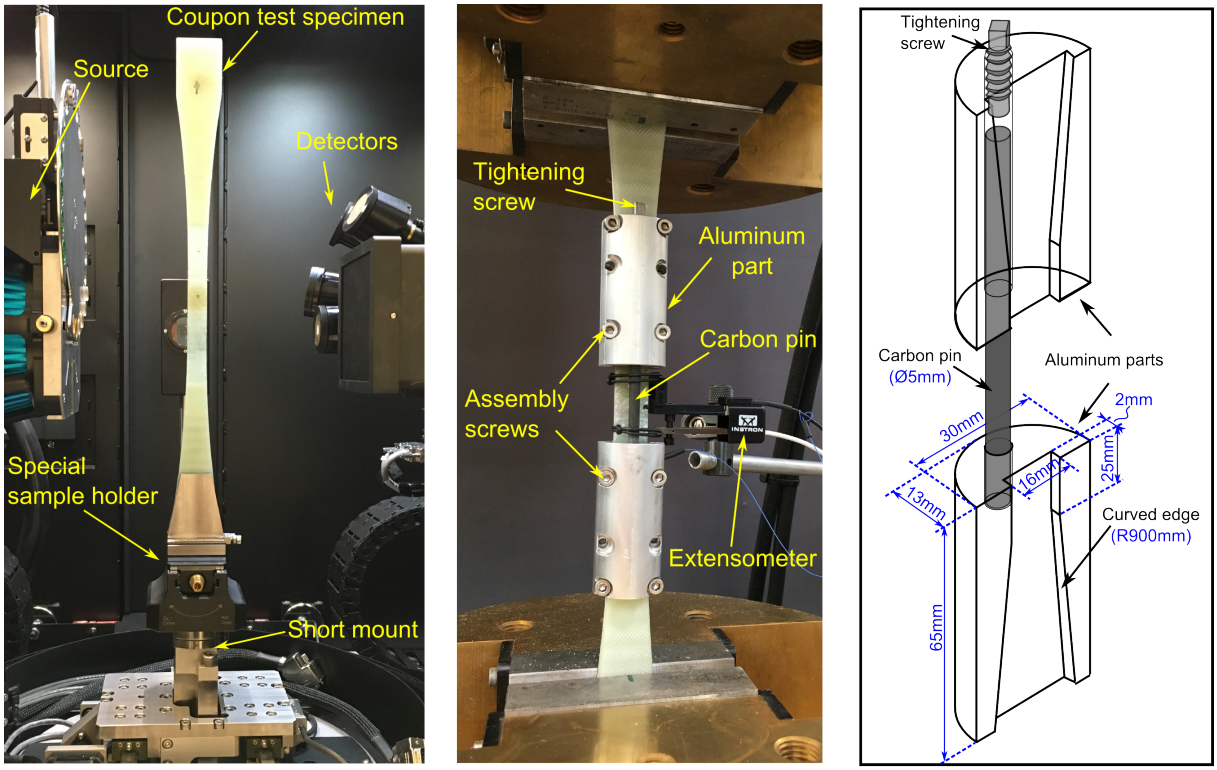

a) Sample mounted in scanner b) Tension clamp on sample c) Principle sketch of clamp tightening mechanism

Figure 1. Specialised experimental setups. a) shows the mounting method for the scanner, b) the tension clamp solution on sample in tension machine, and c) a principle sketch of the tightening mechanism showing half the clamp (scale not exact).

The effect of applied tension on crack visibility was examined using a specially designed tension clamp, which is designed so that the sample can be scanned with the clamp attached. The clamp is shown on the sample in Fig. 1b and Fig. 1c shows a principle sketch of the clamp tightening mechanism along with the approximate dimensions. Fig. 1c only shows half the clamp as it is symmetric, and the holes and assembly screws used to hold the two clamp halves together (seen in Fig. 1b) are excluded for simplicity. While the sample is loaded in a regular tensile test machine, the clamp is mounted on the sample using the assembly screws and the two tightening screws on the top aluminum parts are tightened. By doing so, the carbon pins that transfer the load are also tightened as shown in Fig. 1c. The internal geometry of the aluminium parts of the clamp fits the curvature of the sample, and therefore the aluminum parts are kept in place after the carbon pins are tightened, even after unloading the tensile test machine. That means

that when the load is released on the test machine, the clamp will ensure that the central part of the sample is still in tension. The strain in the sample was measured using an extensometer. The sample was loaded up to 7kN corresponding around 0.2-0.3% strain and then the clamp was mounted on the sample. After removing the load, the clamp stabilised at a strain of 0.17% in the gauge section. Obtaining a higher strain using the clamp was attempted, but even if a higher initial load was used the strain in the gauge section went back to the same value. This could be due to damage in the ends of the carbon pins at high loads, and a slightly modified solution is necessary to obtain higher loads. A possible improvement in the future could be to add reinforcement to the ends of the carbon pins. However, in this study a strain of 0.17% was used, which was the highest obtainable strain for the presented clamp solution.

4. Results and discussion

4.1. Fatigue test result

The measured stiffness degradation of the ex-situ fatigue study is shown by the solid line in Fig. 2a where the four interruption points for CT inspection are marked (N_A-N_D). Slight jumps in the data were observed at each of the interruption points, but since this is due to mounting the extensometers a bit differently every time, the curve sections were off-set to give a continuous curve. Fig. 2a also include two other sets of test data (dashed lines) for a slightly higher strain level (1.1%).

By comparison, it is seen that the shape of the ex-situ fatigue curve is similar to those observed for continuous tests to failure. However, the life-time is less for the ex-situ test performed at 1% strain than for the continuous tests carried out at 1.1% strain, which is opposite of what would be expected. However, Fig. 2b shows the S-N data for samples not affected by X-ray relative to the ex-situ test, and even though the life-time seemed less than for the normal tests, it is not significantly different. Whether this slightly shorter life-time was caused by the effect of X-ray or simply that the sample itself was an outlier cannot be said for certain. However, in addition to the slightly shorter life-time the sample was observed to discolor because of X-ray (Fig. 2c) and it is therefore a subject that requires further investigation.

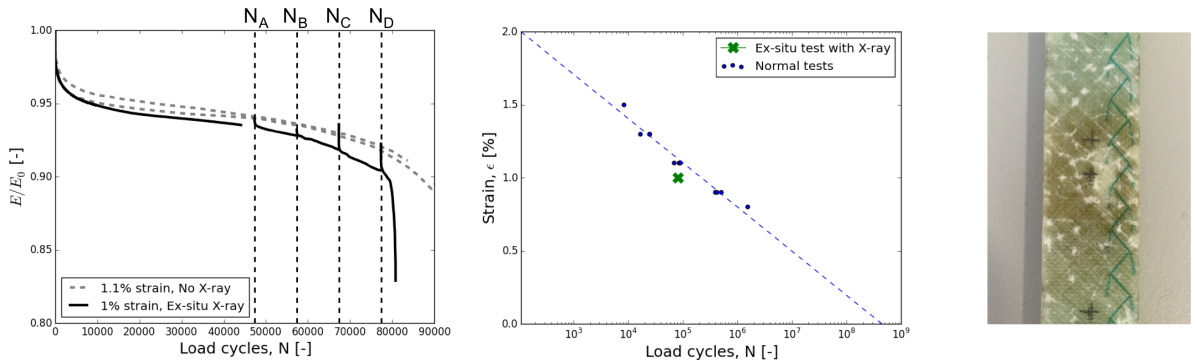

a) Stiffness degradation b) S-N Curve c) Discoloring from X-ray

Figure 2. a) shows the stiffness degradation curve for the ex-situ fatigue test (solid line) and examples of continuous fatigue tests (dashed lines) for samples without X-ray exposure, b) the S-N curve data for samples not affected by X-ray compared to the ex-situ sample, and c) the discoloring observed on the sample after N_D cycles (after all the X-ray experiments).

4.2. Ex-situ X-ray CT monitoring of damage progression

Fig. 3 shows virtual 2D slices of the X-ray CT data (no applied tension) for the four different stages of the fatigue test (N_A-N_D in Fig. 2a). There was a slight variation in the scanned location for each scan because of mounting/dismounting the sample in the holder, however as it is seen from Fig. 3 it is quite a small difference for the scans performed after N_A, N_B, and N_C cycles. The reason for the large variation for the scan performed after N_D cycles was that the bottom of the holder had been disassembled between step N_C and N_D, which is important not to do in future studies. As expected, the UD fibre damage is observed to progress with increasing number of cycles. Both new fibre fractures are observed to appear and the opening

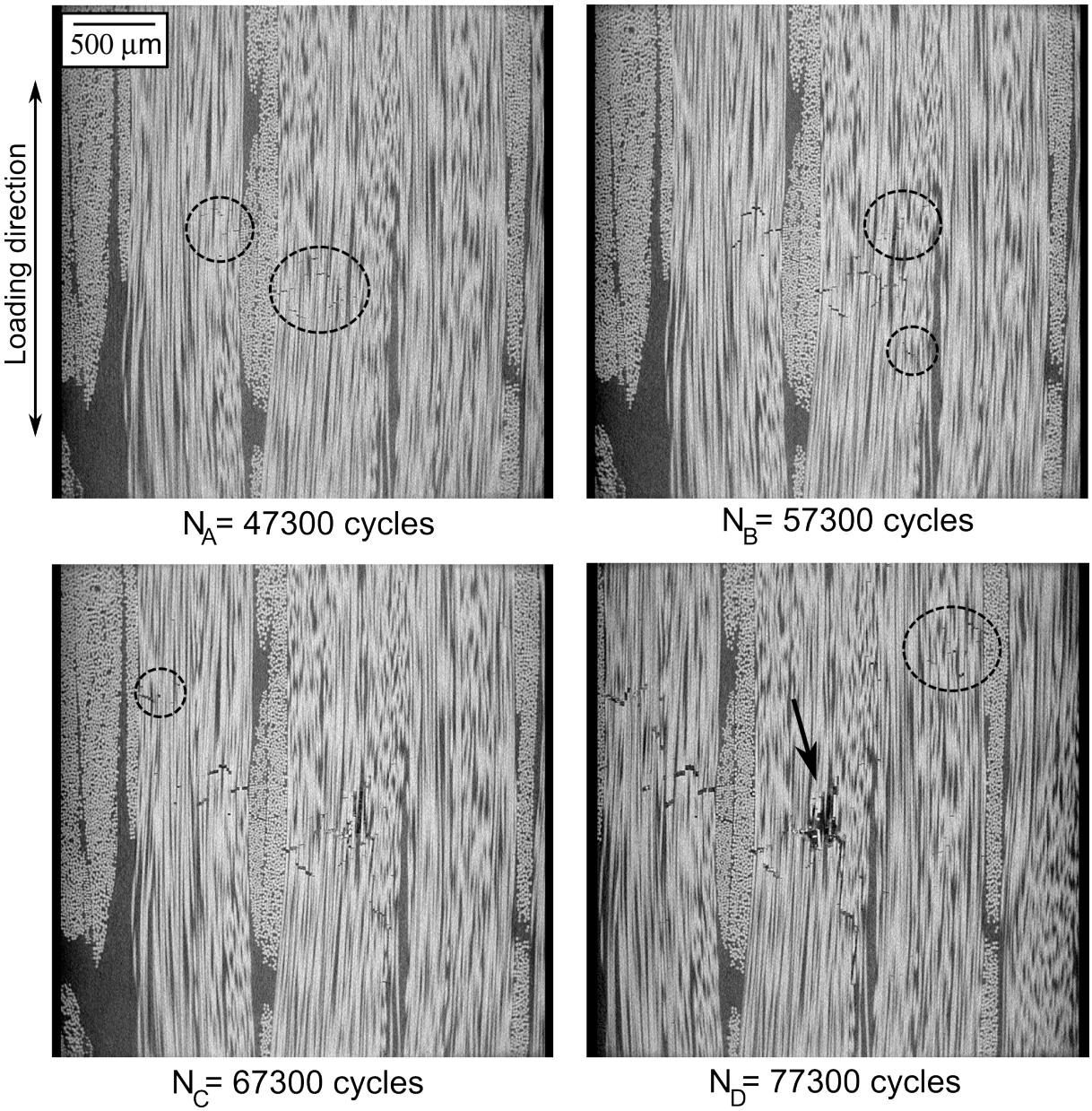

Figure 3. Virtual 2D slice views from 3D X-ray CT scan data showing the damage after each of the four times the fatigue test was interrupted. The ellipses indicate some locations with new damage and the arrow marks a highly damaged region.

of existing fibre fractures is seen to increase for each step. After N_D cycles a damage region with large crack openings compared to other locations was observed (indicated by the arrow in Fig. 3) and the final failure of the sample happened shortly after this (as also seen in Fig. 3). The increasing openings of the UD fibre fractures might be linked of the gradual length increase of the sample during fatigue, however evaluating and comparing the observed damage mechanisms in all the data sets in detail is still ongoing work. In general for all the X-ray data, many fibre fractures were clearly visible, but some had a small opening making them difficult to see. Furthermore, off-axis cracks were not clearly visible because of the small opening. A possible way to increase the visibility of these cracks is to apply tension during scanning in order to open them up, as will be explained in the following section.

4.3. Effect of applied tension during scan

Fig. 4 shows two scans performed in the same damage region of a sample interrupted after 67,000 cycles at 1% strain. Fig. 4a shows a virtual 2D slice from the 3D x-ray data of the unloaded specimen, and Fig. 4b shows the same position with the tension clamp attached keeping the sample at 0.17% strain. It should be noted that 0.17% strain is only around on fifth of the maximum strain during fatigue. Some regions of interest are marked and compared for the loaded sample (region A1-D1) and the unloaded sample (region A2-D2) in Fig. 5.

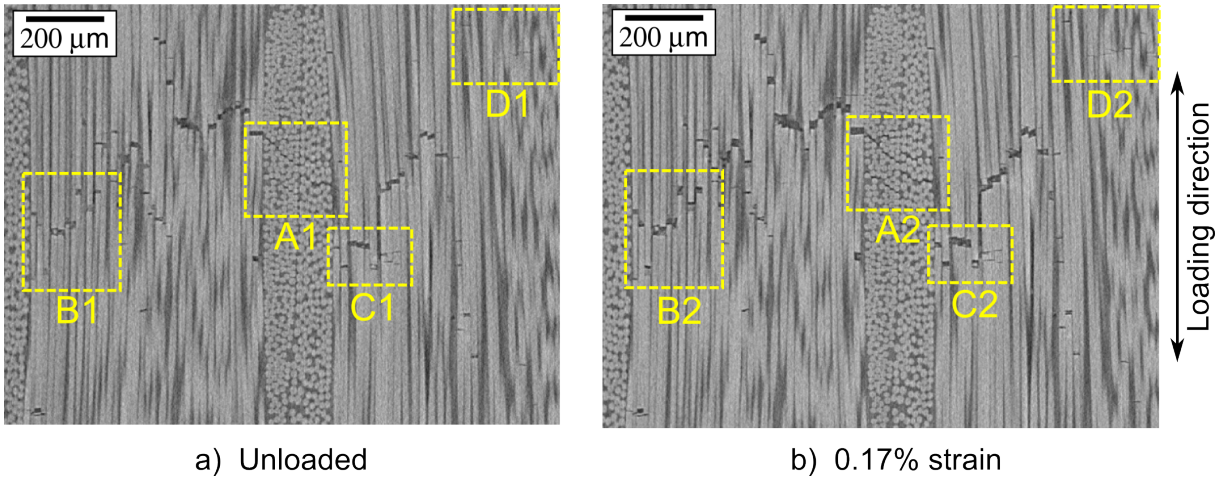

Figure 4. Comparison between observed damage without applied load (a) and with applied load (b). Regions of interest are marked and zoom views can be seen in Fig. 5

By comparing region A1 and A2 in Fig. 5, it is seen that the visibility of the off-axis cracks is only slightly increased at 0.17% strain. The clamp has a larger effect on the visibility of fibre fractures. Some of the fibre fractures are not easy to see without applied tension, whereas they can be seen more clearly with tension (e.g. seen by comparing region B1 and B2). At some locations the opening of the fibre fractures was greatly increased by the tension clamp. In the case of region C1/C2 the opening of some cracks was increased by around a factor two. However, at some locations (e.g. fractures marked by a dashed circle in C2), no change in the opening was observed. There were some locations (e.g. region D1/D2) where the fractures were not visible when the sample was unloaded, whereas they appeared when the sample was strained. The effect of the clamp will be larger if a higher load can be applied, and therefore optimisation of the clamp solution is ongoing work. Furthermore, if an automatic crack counting method was established, it would be possible to quantitatively show the effect of applied tension, and this could also be used to quantify the ex-situ damage. This is currently ongoing work.

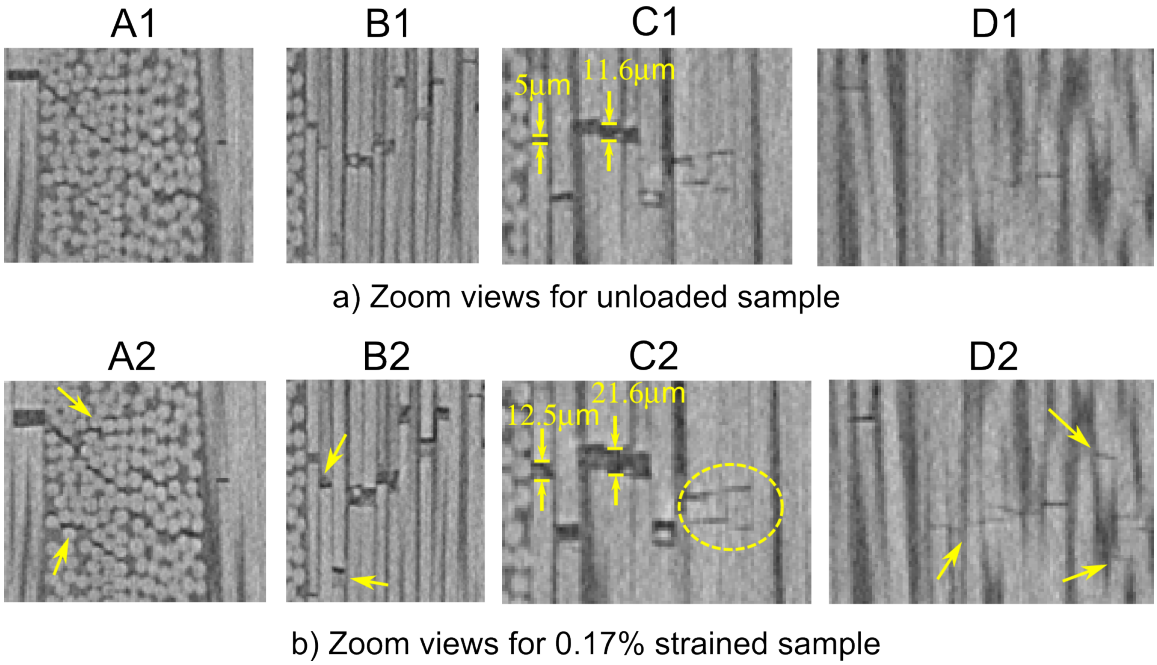

Figure 5. Zoom views in the regions of interest marked in Fig. Fig. 4. a) shows the views for the unloaded sample (A1-D1) and b) the views for loaded sample (A2-D2). The arrows marks some locations with changes when applying load to the sample.

5. Conclusion

In this study, a method for observing fatigue damage progression non-destructively in a glass fibre/polymer coupon test specimens by ex-situ laboratory X-ray CT was explained. Damage was observed in 3D on a micro-structural level including individual fibre fractures and off-axis cracks at four points during the fatigue loading history. The number of fibre fractures along with their opening was seen to increase with increasing number of load cycles. The long time exposure of X-rays on the sample seemed to have a slight negative effect on the tension fatigue life-time, however when scanning four times it did not seem significant. Furthermore, the effect of applying tension during scanning was examined and it was seen that additional fibre fractures and off-axis cracks became visible with load applied. However, it might be necessary to apply a higher strain during scanning to make all the fibre fractures and matrix cracks visible in the X-ray CT images at the considered resolution. Therefore, developing an improved clamp solution is of great interest and is ongoing work.

Acknowledgments

This research was conducted using mechanical testing equipment from DTU Center for Advanced Structural and Material Testing (CASMAT), Grant No. VKR023193 from the Villum Fonden. Financial support from CINEMA: "the allianCe for ImagiNg of Energy MAterials", DSF-grant no. 1305-00032B under "The Danish Council for Strategic Research" is gratefully acknowledged. Additionally, we would like to thank LM Wind Power for manufacturing of test specimens.

References

[1] Nijssen R P L and Brøndsted P 2013 *Advances in Wind Turbine Blade Design and Materials* 175–209
[2] Nijssen R P L 2006 *PhD Thesis, Delt University of Technology*
[3] Zangenberg J, Brøndsted P and Gillespie Jr J W 2014 *Journal of Composite Materials* **48** 2711–2727 ISSN 0021-9983

[4] Jespersen K M, Lowe T, Withers P, Zangenberg J and Mikkelsen L 2016 *Composites Science and Technology* (Submitted)
[5] Pedro F, Márquez G, Mark A, María J, Pérez P and Papaelias M 2012 *Renewable Energy* **46** 169–178
[6] Pereira G F, Mikkelsen L P and McGugan M 2015 *PLOS One* **10** e0141495
[7] Mortell D J, Tanner D A and Mccarthy C T 2014 *Composites Science and Technology* **105** 118–126
[8] Hongwei Z, L M, Brøndsted P, Jinbiao T and Lele G 2010 *Chinese Science Bulletin* **55** 1199–1208
[9] Wright P, Moffat A, Sinclair I and Spearing S M 2010 *Composites Science and Technology* **70** 1444–1452
[10] Scott A E, Mavrigirdati M, Wright P, Sinclair I and Spearing S M 2011 *Composites Science and Technology* **71** 1471–1477
[11] Garcea S C, Macrigirdato M, Scott A E, Sinclair I and Spearing S M 2014 *Composites Science and Technology* **99** 23–30
[12] Garcea S C, Sinclair I and Spearing S M 2015 *Composites Science and Technology* **109** 32–39
[13] Schilling P J, Karedla B P R, Tatiparthi A K, Verges M A and Herrington P D 2005 *Composites Science and Technology* **65** 2071–2078
[14] Sket F, Seltzer R, Molina-Aldareguía J M, Gonzalez C and LLorca J 2012 *Composites Science and Technology* **72** 350–359
[15] Yu B, Blanc R, Soutis C and J W P 2016 *Composites: Part A* **82** 279–290
[16] Pereira G F, Hüther J, Mikkelsen L P and Brøndsted P 2016 *In preparation, DTU Wind Energy*
[17] Zangenberg J 2013 *PhD Thesis, DTU Wind Energy PhD-0018(EN)*